Smoothed Particle Hydrodynamics to Model Spinal Canal Occlusion of a Finite Element Functional Spinal Unit Model under Compression

S. Ngan[1], C. Rampersadh[1], J. Carter[2], and D. S. Cronin[1]
[1] Department of Mechanical and Mechatronics Engineering, University of Waterloo
[2] Origin Forensics LLC

ABSTRACT

Compressive impacts on the cervical spine can result in bony fractures. Bone fragments displaced into the spinal canal produce spinal canal occlusion, increasing the potential for spinal cord injury (SCI). Human body models (HBMs) provide an opportunity to investigate SCI but currently need to be improved in their ability to model compression fractures and the resulting material flow. Previous work to improve fracture prediction included the development of an anisotropic material model for the bone (hard tissues) of the vertebrae assessed in a functional spinal unit (FSU) model. In the FSU model, bony failure was modelled with strain-based element erosion, with a limitation that material that could occlude the spinal canal during compression was removed when an element was eroded. The objective of this study was to implement a multi-physics modelling approach, using smoothed particle hydrodynamics (SPH) with element erosion, to simulate the movement of fractured material during central compression of a C5-C6-C7 cervical spine segment and assess spinal canal occlusion. The calculated maximum occlusion in the original model was 11.1%. In contrast, the enhanced model with SPH had a maximum occlusion of 79.0%, in good agreement with the average experimental maximum occlusion of 69.0% for age-matched specimens. The SPH implementation to preserve fractured material volume enabled the assessment of spinal canal occlusion.

INTRODUCTION

Head-first compressive impacts from events such as vehicle rollovers can lead to bony fractures in the cervical spine. Subsequent spinal compression that projects fractured bone into the spinal canal can result in spinal canal occlusion (Mattucci et al., 2019). Occlusion can compress the spinal cord, leading to possible spinal cord injury (SCI). Human body models (HBMs) provide an opportunity to investigate SCI but currently need to be improved in their ability to model compression fractures and the resulting fractured material flow.

Experiments have sought to quantify the amount of occlusion by measuring the geometric change in the spinal canal area during and after compression of various scales of the spinal column. Two of the methods used to measure occlusion in the cervical spine under central compression

This paper is a student paper from the 18th Injury Biomechanics Symposium and is published in a special issue of SAE International Journal of Transportation Safety.
It is preliminary work, has not been peer reviewed, and should not be cited because it is a work in progress.

were the use of an occlusion transducer (Chang et al., 1994; Carter et al., 2000) and of a spinal canal occlusion transducer (SCOT) (Carter, 2002; Nuckley et al., 2007). The occlusion transducer consisted of a closed-loop fluid-filled tube system. The polymer tube of the occlusion transducer was fitted into the spinal canal. As the specimen was compressed and fractured, bone fragments would push on the tube, causing it to narrow. The narrowing of the tube would result in a pressure drop measured by a pressure transducer, which would be used to calculate a percent occlusion in terms of the change in canal cross-sectional area (Chang et al., 1994) or midsagittal canal diameter (Carter et al., 2000) of the spinal canal. One of these experiments looked at burst fractures from compression of the cervical spinal and reported the peak percent occlusion to be 71% (Carter et al., 2000). The SCOT used a polymer tube filled with a saline solution fitted through the spinal canal. An electrical current was passed through the tube. As bone fragments caused the tube to narrow, the voltage drop was used to calculate the percent occlusion in terms of a change in canal cross-sectional area (Raynak et al., 1998) or midsagittal canal diameter (Carter, 2002). The experiments looking at the compression of functional spinal unit (FSU) segments using a SCOT reported average maximum percent occlusions during loading of 52% to 59% (Carter, 2002; Nuckley et al., 2007).

A contemporary HBM, the Global Human Body Models Consortium (GHBMC) average-stature male model (M50) with a detailed neck model (Barker et al., 2017), was developed to investigate crash-induced injuries (CIIs) (DeWit and Cronin, 2012). Previous work to improve fracture prediction included the development of an anisotropic material model for the hard tissues of the vertebrae, assessed in a functional spinal unit (FSU) model (Khor et al., 2017). In the FSU model, hard tissue failure was modelled with strain-based element erosion, with a limitation that material and energy were removed when an element was eroded. Thus, the model did not represent fractured hard tissue that could occlude the spinal canal during compression. Therefore, the objective of this study was to implement a multi-physics modelling approach using smoothed particle hydrodynamics (SPH) with element erosion to simulate the movement of fractured material during compression and assess spinal canal occlusion.

METHODS

Model Set-Up

A two-FSU segment from the lower cervical spine (C5-C6-C7) was extracted from the GHBMC HBM (M50-O v6.0). The FSU segment included the cortical and trabecular bone of the vertebrae, endplates, intervertebral discs, facet joint cartilages, and ligaments (Barker et al., 2022). As reported in experimental testing, a central compression boundary condition was applied (Carter et al., 2002; Khor et al., 2015). The inferior C7 vertebra was contained in the bottom potting, which was fully constrained. The superior C5 vertebra was contained in the top potting, which was displaced downward in compression by an initial 40.0 N pre-load followed by three phases of displacement. The first displacement phase loaded the segment using a displacement pulse to achieve a maximum displacement of 15.0 mm over 16.0 ms. The second displacement phase was a holding phase, in which the top potting was held at 14.2 mm of displacement. The final

This paper is a student paper from the 18th Injury Biomechanics Symposium and is published in a special issue of SAE International Journal of Transportation Safety.
It is preliminary work, has not been peer reviewed, and should not be cited because it is a work in progress.

displacement phase was the unloading phase, where the top potting was unloaded to 7.6 mm of displacement.

Trabecular Bone Properties and SPH Implementation

SPH was implemented into the trabecular bone to enhance the occlusion response from the fracture of the vertebrae. The solid Lagrangian elements of the trabecular bone were assigned an anisotropic foam material model (Khor et al., 2015). The solid elements failed using a strain-based element erosion criterion with critical strain values of 0.9 in compression and 0.09 in tension. To implement the SPH, a solid Lagrangian trabecular bone element would be transformed into one SPH particle upon reaching a critical strain value. Since the activated SPH particles represented the compacted and densified fragments of the fractured trabecular bone, the material property values of the elastic material model of the SPH particles were based on the properties of the solid Lagrangian elements of the trabecular bone.

Occlusion Evaluation

To assess the effect of the SPH implementation on modelling occlusion, two models were simulated and evaluated for occlusion. The No SPH Model only included strain-based element erosion to model fracture. The SPH Model included the SPH implementation where SPH particles activated upon erosion. Occlusion was then evaluated at each time step. The occlusion of the simulation results was determined using an image of the C6 vertebra in the coronal plane viewed from the superior to inferior direction. From this image, a rectangle was drawn around the spinal canal to include the spinal canal space at the beginning of the simulation. The area within the rectangle occupied by hard tissue was measured using ImageJ, an image processing program. Using the measured areas, the occlusion values throughout the simulation were expressed as a percent of the initial spinal canal area. The maximum measured percent occlusion from the simulation was compared to the maximum occlusion reported from experimental results.

RESULTS

The percent occlusions measured for the No SPH Model and the SPH Model were initially in agreement before diverging after fracture occurred in the pedicles (Figure 1). At the start of loading, the percent occlusion increased by 1.4% as the segment was compressed (Figure 1, Point A to B). This corresponded to the deformation of the intervertebral discs and sliding between vertebrae at the facet joints. As the pedicles fractured, the C6 vertebral body rotated, displacing the superior edge of the vertebral body into the spinal canal. The movement of the C6 vertebral body into the spinal canal corresponded to an increase in occlusion to 8.0% occlusion (Figure 1, Point B to C). As fracture and erosion progressed to the articular pillar of the C6 vertebra and the C5 and C7 vertebral bodies, the percent occlusion of the No SPH Model and the SPH Model followed a similar increase before diverging (Figure 1, Point D).

This paper is a student paper from the 18th Injury Biomechanics Symposium and is published in a special issue of SAE International Journal of Transportation Safety.
It is preliminary work, has not been peer reviewed, and should not be cited because it is a work in progress.

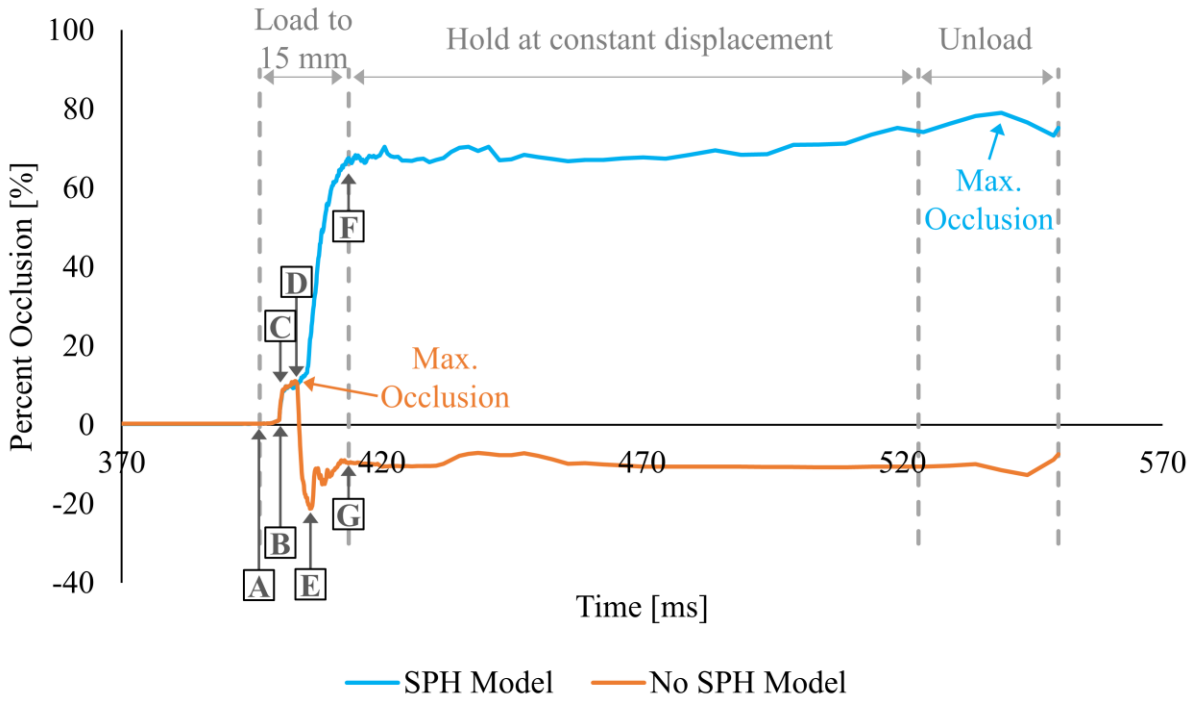

Figure 1: Occlusion as a function of time from simulation.

In the No SPH Model, a decrease in percent occlusion was observed as the posterior part of the C6 vertebra (articular pillar, lamina, and spinous process) moved in the posterior direction, owing to fracture of the lateral processes after reaching a maximum percent occlusion of 11.1% (Figure 1, Point D). The anterior movement of the articular pillar, lamina, and spinous process occurred after fracture (erosion) progressed along the inferior surface of the articular pillar. As these parts of the vertebra moved away from the spinal canal, the percent occlusion correspondingly decreased to a percent occlusion of -21.2% (Figure 1, Point E). The negative values of percent occlusion indicated a larger spinal canal space compared to the spinal canal at the beginning of the simulation. The percent occlusion then increased to -9.6% as the fracture propagated through the vertebral body, displacing bone material into the spinal canal (Figure 1, Point G). The increase in percent occlusion from -21.2% to -9.6% corresponded to a decrease in the spinal canal area; however, the area in the spinal canal was still larger than the spinal canal space at the beginning of the simulation. After loading, as the displacement was held constant, the average percent occlusion was -9.7%.

In contrast to the decrease in percent occlusion of the No SPH Model, the implementation of SPH in the SPH Model resulted in an overall increase in percent occlusion as the cervical spine segment was compressed (Figure 1, Point D to F). As fracture progressed in the articular pillars, superior C5 vertebra, and inferior C7 vertebra, the percent occlusion increased due to the movement of the C6 lamina and spinous process in the anterior direction. As fracture propagated in the C6 vertebral body, both the C6 vertebral body and lamina were pushed into the spinal canal, contributing to the increase in occlusion until the maximum displacement (Figure 1, Point F). Furthermore, the SPH Model had bone fragments, represented by the SPH particles, in the spinal canal. The movement of these bone fragments into the spinal canal also contributed to the increase

This paper is a student paper from the 18th Injury Biomechanics Symposium and is published in a special issue of SAE International Journal of Transportation Safety.
It is preliminary work, has not been peer reviewed, and should not be cited because it is a work in progress.

in percent occlusion. At the maximum displacement, a percent occlusion of 67.6% was measured. After loading, the average occlusion was 68.1% when the displacement was held constant. The largest percent occlusion of 79.0% was measured during the unloading phase in SPH Model. The increase in occlusion seen during the unloading phase of the SPH Model occurred as an artifact of the simulation as the solid Lagrangian elements of the trabecular bone went through large unphysical deformations and as SPH particles moved through the spinal canal space.

DISCUSSION

The implementation of SPH contributed to the difference in the direction of movement of the lamina and spinous process in the No SPH Model and the SPH Model. The point where the trends in percent occlusion diverged (Figure 1, Point D) corresponded to the progression of fracture (erosion) in the inferior region of the articular pillar. The region of erosion was along the load path between the C5 to C6 and C6 to C7 facet joint contact points. In the No SPH Model, the erosion led to a loss of material and therefore structural support along this load path. Thus, as the segment was compressed, the articular pillars of the C6 vertebra were allowed to rotate and slide in the posterior direction. The C6 lamina and spinous processes moved posteriorly with the articular pillars leading to a decrease in percent occlusion as the hard tissue of the C6 vertebra moved away from the spinal canal. In contrast, in SPH Model, the activated SPH particles provided structural support as the inferior region of the C6 articular pillars fractured (eroded). Thus, rotation of the C6 articular pillars was prevented. As the cervical spine segment was compressed and the contact points between facet joints shifted, the C6 articular pillar was instead pushed in the anterior direction. The lamina and the spinous process moved anteriorly with the articular pillars leading to the increase in percent occlusion as hard tissue moved into the spinal canal (Figure 2).

This paper is a student paper from the 18th Injury Biomechanics Symposium and is published in a special issue of SAE International Journal of Transportation Safety.
It is preliminary work, has not been peer reviewed, and should not be cited because it is a work in progress.

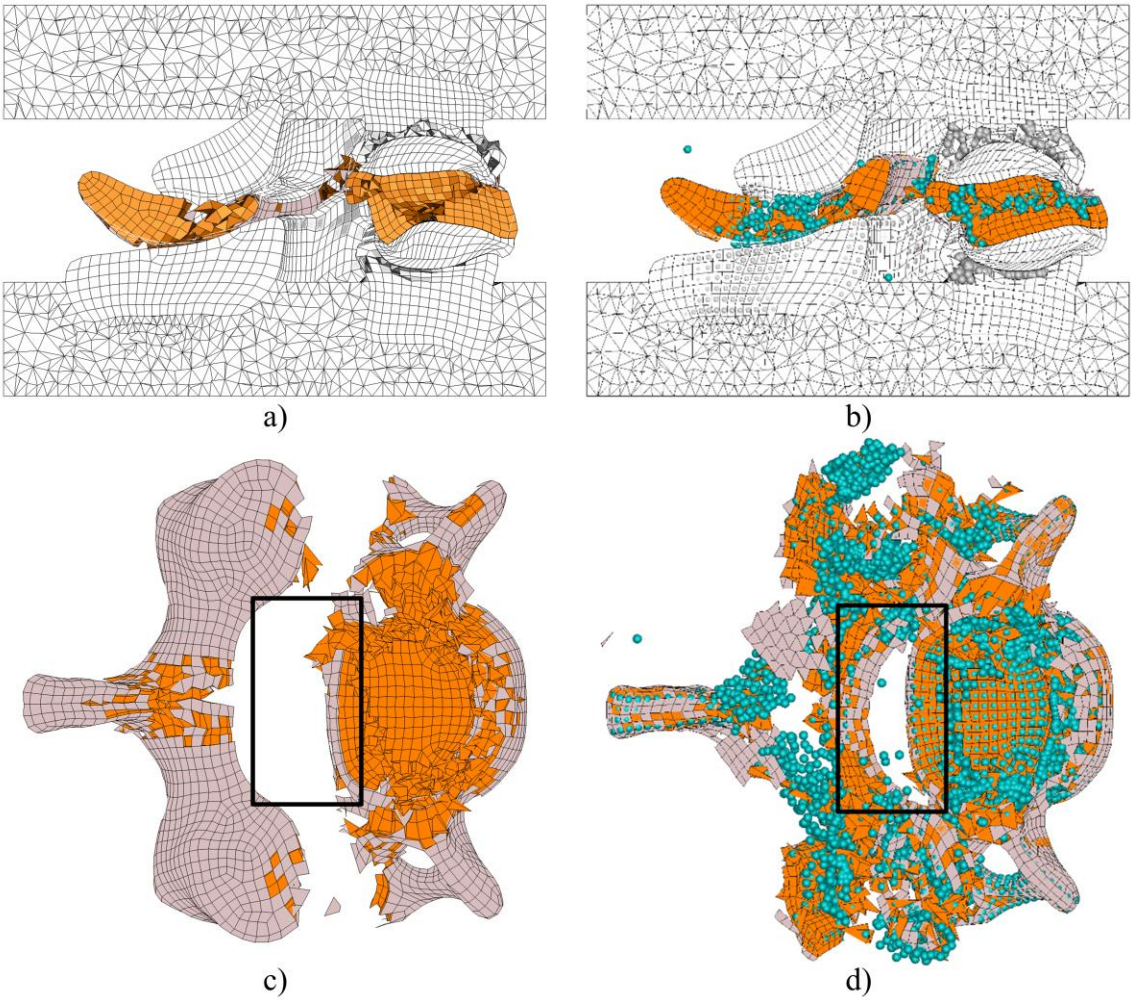

Figure 2: Sagittal view of the segment at maximum displacement (Figure 1, Point A) for a) the No SPH Model and b) the SPH Model. Coronal view of the C6 vertebra for c) the No SPH Model and d) the SPH Model. The cyan spheres are the SPH particles, the orange elements are the trabecular bone elements, and the light purple elements are the cortical bone elements. The black rectangle represents the area of interest, including the spinal canal space at the beginning of the simulation before preload and displacement were applied.

In both the No SPH Model and the SPH Model, the superior half of the C6 vertebral body was pushed into the spinal canal, contributing to an increase in percent occlusion up to Point D (Figure 1). The movement of the C6 vertebral body began with the initiation and then propagation of fracture in the C6 vertebral body. Once the vertebral body fractured, fragments from the superior C6 vertebral body were displaced into the canal (Figure 2 a and b). The implementation of SPH to preserve vertebral body material during fracture contributed to the fragments from the superior C6 vertebral body displacing about 0.7 mm more into the spinal canal compared to the No SPH Model.

The SPH particles in the spinal canal led to the higher measured percent occlusion (Figure 2). Due to the mesh-free nature of the SPH particles, these elements are free to move in the same

This paper is a student paper from the 18th Injury Biomechanics Symposium and is published in a special issue of SAE International Journal of Transportation Safety.
It is preliminary work, has not been peer reviewed, and should not be cited because it is a work in progress.

manner as comminuted or fractured material, facilitating the flow of bone fragments into the spinal canal during the impact simulation.

The occlusion measured in the SPH Model was higher than in the No SPH Model (Table 1). Without the SPH implementation, the maximum occlusion of 11.1% was less than the average experimental maximum occlusion of 58.7% from the experimental specimen of all ages and sexes. In the SPH Model, the maximum percent occlusion increased to 79.0%. Although this value is greater than the experimental average, it agrees with reported experimental averages of 69.0% for average-stature male specimens (Carter, 2002) and 71% for burst fractures in the cervical spine (Carter et al., 2000). Thus, the implementation of SPH allowed more hard tissue material to be pushed into the spinal canal resulting in higher occlusion values, similar to experimentally reported values for maximum percent occlusion.

Table 1: Key percent occlusion values

Occlusion Value Type	**Experimental Average (Carter, 2002)**	**Model Simulation**	
		No SPH Model	**SPH Model**
Maximum Occlusion [%]	58.7±7.5	11.1	79.0
Occlusion at Maximum Displacement [%]	58.7	-9.6	67.6

Limitations

While the percent occlusion value of the model with the SPH implementation was closer to the experimental average, the percent occlusion was greater than the experimental average for maximum occlusion. One factor that contributed to the increased occlusion measured from the model simulation was the absence of the polymer tube used in the experiments to measure occlusion. The tube in the experiments may have provided resistance, preventing some of the bone fragments from displacing into the canal of the experimental specimen. Since the polymer tube was not present in the model, this resistance was not modelled. Therefore, bone fragments, such as those represented by the SPH particles, were free to flow into the canal and contribute to an increase in the percent occlusion measurement.

One of the limitations of the model was its ability to predict spinal canal occlusion during the unloading of the FSU segment. Unlike the occlusions measured from the FSU segment model, the experimental maximum occlusions occurred at the maximum displacement. Furthermore, the experimental percent occlusion decreased as the experimental specimens were unloaded. In the FSU segment model simulation, the maximum occlusion occurred during loading for the No SPH Model and during unloading for the SPH Model. In the SPH Model, after the steep increase in percent occlusion during loading, the percent occlusion increased by another 11.4% even as the displacement decreased. The lack of bone marrow in the trabecular bone and additional connective tissue in the model contributed to the different unloading responses between the experiments and the model. The connective tissues in the FSU segment model were the cervical ligaments modelled using two-dimensional beam elements. The two-dimensional representation of the cervical ligaments resulted in a lack of confinement of other tissues in the cervical spine that would be

This paper is a student paper from the 18th Injury Biomechanics Symposium and is published in a special issue of SAE International Journal of Transportation Safety.
It is preliminary work, has not been peer reviewed, and should not be cited because it is a work in progress.

present with a three-dimension cervical ligament structure. Thus, while the cervical ligaments contributed to pulling the bone fragments back out of the spinal canal during the unloading of the experimental specimen, this phenomenon was not observed in the model. The decrease in occlusion as unloading occurs is, therefore, not modelled.

CONCLUSIONS

With the implementation of the SPH, trabecular bone material was preserved post-fracture. The preserved material, modelled by SPH particles, allowed hard tissue material to flow into the spinal canal. The hard tissue material in the spinal canal enabled the assessment of spinal canal occlusion. Future work will look at integrating the spinal cord into the spinal canal.

ACKNOWLEDGEMENTS

The authors gratefully acknowledge the Global Human Body Models Consortium, the Natural Sciences and Engineering Research Council of Canada, Stellantis Canada, GM Canada, and Honda Development and Manufacturing of America for financial support of this research, and the Digital Alliance of Canada for providing the necessary computing resources.

REFERENCES

BARKER, J.B., CRONIN, D.S., NIGHTINGALE, R.W. (2017). Lower Cervical Spine Motion Segment Computational Model Validation: Kinematic and Kinetic Response for Quasi-Static and Dynamic Loading. Journal of Biomechanical Engineering 139. https://doi.org/10.1115/1.4036464

BARKER, J., CRONIN, D.S. (2022). Muscle Activation Affects Kinematic Response and Injury Risk in Non-Traditional Oblique Impact Scenarios Assessed with a Head and Neck Finite Element Model. SAE International Journal of Transportation Safety 10.

CARTER, J.W. (2002). Compressive cervical spine injury: The effect of injury mechanism on structural injury pattern and neurologic injury potential. PhD Dissertation.

CARTER, J.W., KU, G.S., NUCKLEY, D.J., CHING, R.P. (2002). Tolerance of the cervical spine to eccentric axial compression. Stapp Car Crash J 46, 441–459. https://doi.org/10.4271/2002-22-0022

CARTER, J.W., MIRZA, S.K., TENCER, A.F., CHING, R.P. (2000). Canal Geometry Changes Associated With Axial Compressive Cervical Spine Fracture. Spine 25, 46.

This paper is a student paper from the 18th Injury Biomechanics Symposium and is published in a special issue of SAE International Journal of Transportation Safety.
It is preliminary work, has not been peer reviewed, and should not be cited because it is a work in progress.

DEWIT, J.A., CRONIN, D.S. (2012). Cervical spine segment finite element model for traumatic injury prediction. Journal of the Mechanical Behavior of Biomedical Materials 10, 138–150. https://doi.org/10.1016/j.jmbbm.2012.02.015

KHOR, F., CRONIN, D. (2015). Constitutive Modeling of Cortical and Trabecular Bone Applied to Compression Loading and Failure of a Lower Cervical Spine Segment Model. Presented at the 2016 Injury Biomechanics Symposium.

KHOR, F., CRONIN, D., CARTER, J. (2018). Hard Tissue Failure of an Aged Lower Cervical Spine Segment Model in Compression Loading with Anterior-Posterior Eccentricity. Presented at the 2018 Injury Biomechanics Symposium.

KHOR, F., CRONIN, D., VAN TOEN, C. (2017). Lower Cervical Spine Hard Tissue Injury Prediction in Axial Compression, in: IRCOBI Conference Proceedings. Presented at the 2017 International Research Council on Biomechanics of Injury (IRCOBI).

MATTUCCI, S., SPEIDEL, J., LIU, J., KWON, B.K., TETZLAFF, W., OXLAND, T.R. (2019). Basic biomechanics of spinal cord injury — How injuries happen in people and how animal models have informed our understanding. Clinical Biomechanics, SI: Central Nervous System (CNS) Injury Biomechanics 64, 58–68. https://doi.org/10.1016/j.clinbiomech.2018.03.020

This paper is a student paper from the 18th Injury Biomechanics Symposium and is published in a special issue of SAE International Journal of Transportation Safety.
It is preliminary work, has not been peer reviewed, and should not be cited because it is a work in progress.